Journal of Cancer Research and Clinical Oncology (2019) 145:2675–2687
https://doi.org/10.1007/s00432-019-03026-7

ORIGINAL ARTICLE – CANCER RESEARCH

Inhibition of bone morphogenetic protein signaling reduces viability, growth and migratory potential of non-small cell lung carcinoma cells

Jelena Mihajlović[1] · Laura A. M. Diehl[1] · Andreas Hochhaus[1] · Joachim H. Clement[1]

Received: 19 February 2019 / Accepted: 11 September 2019 / Published online: 17 September 2019

Abstract

Purpose BMP signaling has an oncogenic and tumor-suppressing activity in lung cancer that makes the prospective therapeutic utility of BMP signaling in lung cancer treatment complex. A more in-depth analysis of lung cancer subtypes is needed to identify BMP-related therapeutic targets. We sought to examine the influence of BMP signaling on the viability, growth and migration properties of the cell line LCLC-103H, which originates from a large cell lung carcinoma with giant cells and an extended aneuploidy.

Methods We used BMP-4 and LDN-214117 as agonist/antagonist system for the BMP receptor type I signaling. Using flow cytometry, wound healing assay, trans-well assay and spheroid culture, we examined the influence of BMP signaling on cell viability, growth and migration. Molecular mechanisms underlying observed changes in cell migration were investigated via gene expression analysis of epithelial–mesenchymal transition (EMT) markers.

Results BMP signaling inhibition resulted in LCLC-103H cell apoptosis and necrosis 72 h after LDN-214117 treatment. Cell growth and proliferation are markedly affected by BMP signaling inhibition. Chemotactic motility and migratory ability of LCLC-103H cells were clearly hampered by LDN-214117 treatment. Cell migration changes after BMP signaling inhibition were shown to be coupled with considerable down-regulation of transcription factors involved in EMT, especially Snail.

Conclusions BMP signaling inhibition in LCLC-103H cells leads to reduced growth and proliferation, hindered migration and accelerated cell death. The findings contribute to the pool of evidence on BMP signaling in lung cancer with a possibility of introducing BMP signaling inhibition as a novel therapeutic approach for the disease.

Keywords BMP signaling · BMP-4 · Large cell lung carcinoma cell line · Live cell imaging · Snail

Introduction

Lung cancer is the leading cause of cancer-related mortality worldwide, responsible for nearly 20% of cancer-related deaths (Ferlay et al. 2015). Therapeutic approach for lung cancer depends on the histological type (immunohistochemical markers) and stage of the disease (Brandao et al. 2012; Reungwetwattana et al. 2012). Despite great progress in developing new targeted therapies, 5-year survival rate of 10–15% for lung cancer patients is still very low (Ferlay et al. 2018). Lung cancer remains the cancer with the highest mortality rate worldwide, underlying the need for innovative drug development and detection of novel therapeutic targets for the disease.

Bone morphogenetic proteins (BMPs) are multifunctional cytokines that belong to transforming growth factor β (TGFβ) superfamily of growth and differentiation factors. They are ubiquitously expressed in human body and play an essential role in embryonic development and in homeostasis of adult organism. BMPs fulfill their biological function through activation of canonical SMAD-dependent signaling pathway. The pathway includes serine/threonine kinases, forming receptor tetramers consisting of two type I and two type II BMP receptors. Upon ligand binding, constitutively active type II receptor transphosphorylates type I receptor, which in turn phosphorylates receptor-regulated SMADs (R-SMADs-SMAD1/5/8(9)). Subsequently, the

Electronic supplementary material The online version of this article (https://doi.org/10.1007/s00432-019-03026-7) contains supplementary material, which is available to authorized users.

✉ Joachim H. Clement
joachim.clement@med.uni-jena.de

[1] Klinik Innere Medizin II, Abteilung Hämatologie und Internistische Onkologie, Universitätsklinikum Jena, Am Klinikum 1, 07747 Jena, Germany

phosphorylated R-SMADs are in complex with SMAD4 (Co-SMAD) and translocate into the nucleus. Transcriptional regulation of BMP target genes includes direct binding of the complex to DNA, or through interaction of the complex with DNA-binding proteins, transcriptional coactivators or corepressors. In this way, BMPs control transcription of a wide range of genes, e.g., *SMAD6*, *Bambi, Vent2, SMAD7, hepcidin*, as well as *Runx*, *Msx* and *ID* gene families (Clement et al. 2000; Hollnagel et al. 1999; Miyazono et al. 2010). BMPs can signal through other SMAD-independent pathways, including activation of mitogen-activated protein kinases (MAPK)-ERK, JNK or P38 MAPK, and PI3K/AKT signaling.

BMP-4 is a member of BMP subfamily whose importance in development of bone, heart, intestines, lung, brain and kidney has been described in detail (Bellusci et al. 1996; Bénazet et al. 2009; Danesh et al. 2009; Haramis et al. 2004; Miyazaki et al. 2003; Robert 2007; Sadlon et al. 2004; Winnier et al. 1995). BMP-4 is expressed in a subset of normal adult tissues where it likely contributes to tissue homeostasis. Recently, it has been implied that BMP-4 may play a critical role in development and progression of various cancer types (Alarmo et al. 2013; Thawani et al. 2010; Zhang et al. 2016). *BMP-4* gene mutations have been related to BMP-4 overexpression and found to predispose to colorectal cancer (Lubbe et al. 2012). The expression of BMP-4 in sporadic cancer is reported to be diverse, depending on cancer type and subtype. In lung cancer, BMP-4 protein expression was found to be significantly higher in non-small cell lung carcinoma (NSCLC) than in small cell lung carcinoma (SCLC) tissues, showing also differences in the expression level among NSCLC subtypes (Alarmo et al. 2013). Here, the expression of BMP-4 is shown to be significantly higher in adenocarcinoma and large cell lung carcinoma than in squamous cell lung carcinoma biopsies.

BMP-4 is involved in the regulation of cancer cell growth, migration, invasion, differentiation, apoptosis, and angiogenesis (Kallioniemi 2012). The available data report conflicting findings with regard to the functional implications of the BMP-4 signaling. On one hand, BMP-4 is described to inhibit growth in lung (Buckley et al. 2004; Fang et al. 2014; Su et al. 2009), breast (Ampuja et al. 2013), pancreatic (Virtanen et al. 2011), gastric carcinoma (Shirai et al. 2011), and retinoblastoma (Müller et al. 2015) cells. On the other hand, there is evidence on stimulatory or at least no inhibitory effect of BMP-4 signaling on cell growth, as shown on melanoma (Rothhammer et al. 2005), colon cancer (Deng et al. 2009), hepatocellular carcinoma (Maegdefrau et al. 2009), ovarian cancer (Shepherd and Nachtigal 2003), and again retinoblastoma (Haubold et al. 2010) cells. Literature on the impact of BMP-4 on the induction of apoptosis in different cancer cell lines is also controversial. Further, BMP-4 is frequently suggested as a strong inducer of cancer cell migration, invasion, and epithelial–mesenchymal transition (Alarmo and Kallioniemi 2010; Ampuja et al. 2016; Buckley et al. 2004; Guo et al. 2012; Shirai et al. 2011; Virtanen et al. 2011). Due to the low number of studies and diversity of experimental designs used for elucidating BMP-4 activity, it remains unclear whether the discrepancies are caused by cell-line specific differences and/or tissue-specific variability (Kallioniemi 2012).

In this work, we sought to investigate the impact of BMP signaling on the behavior of poorly differentiated NSCLC [formally denominated as large cell lung carcinoma (LCLC)]. The study was focused on examining the implications of BMP signaling on the viability, growth and migration properties of the LCLC-103H cells. A specific BMP signaling inhibitor, LDN-214117 and BMP-4, as a prominent representative of the BMP family, was used. The ultimate goal was to generate experimental data on BMP signaling in this rather infrequently exploited lung cancer subtype, contributing to the experimental pool of evidence on the potential introduction of BMP signaling as a therapeutic target in lung cancer.

Materials and methods

Cell culture

The lung carcinoma cell line LCLC-103H was purchased from the Leibniz Institute DSMZ-German Collection of Microorganisms and Cell Cultures (Braunschweig, Germany). The cell line was established from a pleural effusion of a non-small cell lung carcinoma histologically classified as large cell carcinoma with giant cells (Bepler et al. 1988). Cells were cultivated at 37 °C in a humidified atmosphere with 5% CO_2, in RPMI 1640 + Gluta-MAX-I (Thermo Fisher Scientific, Waltham, MA, USA) medium (hereafter referred to as RPMI) supplemented with 10% FCS (Biochrom GmbH, Berlin, Germany). For generating transient GFP-expressing cells, $2*10^6$ LCLC-103H cells were transferred into a 15 mL CELLSTAR® Centrifuge Tube (Greiner Bio-One GmbH, Frickenhausen, Germany) and centrifuged for 5 min at 200 rcf. The medium was removed and cells were resuspended in 100 µL Amaxa-Solution V according to the protocol AMAXA® Cell Line Nucleofactor® KiT V (Lonza Group AG, Basel, Switzerland). The cells were transfected with 2 µg pmaxGFP® Vector and grown for 1 day in a humidified atmosphere at 37 °C containing 5% CO_2. Cell line was regularly confirmed mycoplasma-free using commercially available PCR-based Venor™ GeM Mycoplasma Detection Kit (Sigma-Aldrich Chemie GmbH, Steinheim, Germany).

Western blot analysis

LCLC-103H cells were seeded in 6-well cell culture plates in concentration of 1.5×10^5 cells/well in RPMI+10% FCS medium. After overnight incubation, the cells were starved for 12–16 h in serum-free RPMI medium. Treatments were performed in serum-free RPMI medium with 2, 50 and 100 ng/ml BMP-4 (Thermo Fisher Scientific) and 5 µM LDN-214117 (Sigma-Aldrich). Control group of cells was incubated in serum-free RPMI medium and appropriate volume of vehicle for both BMP-4 and LDN-214117—4 mM HCl with 0.1% BSA and DMSO, respectively. Cells were lysed in 100 µl Triton-X lysis buffer (see Supplement Table S1). Protein concentration of the cell lysates was determined using Bradford reagent (Sigma-Aldrich). For SDS-PAGE, 15 µg of total protein per lane was used. Each sample was loaded on Criterion™ XT 4–12% Bis–Tris polyacrylamide gel (BioRad Laboratories GmbH, München, Germany). The blotting process was performed using Trans-Blot Turbo Transfer System (BioRad) with a ready-to-use transfer pack including buffer, filter paper and PVDF membrane. Primary antibodies used include rabbit anti-phospho-Smad1 (Ser463/465)/Smad5 (Ser463/465)/Smad9 (Ser465/467) (Cell Signaling Technology, Danvers, MA, USA, 1:1000 dilution), rabbit anti-Smad1 (Cell Signaling Technology, 1:1000 dilution), rabbit anti-Id1 (C-20) (Santa Cruz Biotechnology, Dallas, TX, USA, 1:1000 dilution), rabbit anti-GAPDH (Abcam, Cambridge, United Kingdom, 1:5000 dilution). Secondary antibody used was goat anti-rabbit IgG-HRP (Santa Cruz Biotechnology, 1:5000 dilution). Protein bands were detected using Immobilon™ Western Chemiluminescent HRP Substrate (Merck Millipore, Billerica, MA, USA) and visualized on the ImageQuant LAS 4000. Developed blots were analyzed semi-quantitatively using the ImageJ 1.50e software (Wayne Rasband, National Institutes of Health, Bethesda, MD, USA).

Cell viability assay

LCLC-103H cells were seeded in T25 cell culture flasks in concentration of 1.5×10^5 cells/flask in RPMI+10% FCS medium and incubated overnight under standard incubation conditions (37 °C, 5% CO_2). Next day, treatments were performed in RPMI + 1% FCS medium and appropriate amount of BMP-4, LDN-214117 or vehicle. Effects of BMP-4 and LDN-214117 on the viability of LCLC-103H cells were observed 24, 48, 72 and 96 h after the treatments. Cells were incubated for 20 min in 100 µl staining solution consisting of APC-conjugated annexin-V (BD Biosciences, Singapore, 1:25 dilution) and propidium iodide (50 µg/ml, BD Biosciences, 1:25 dilution), at RT in the dark. Data were acquired on BD FACSCalibur™ system, measuring 10^4 events/sample; data analysis was performed using FlowJo® software (FLOWJO, LLC, Ashland, OR, USA).

Cell growth assay

LCLC-103H cells were seeded in a 24-well cell culture plate in RPMI+10% FCS medium at density of 4×10^4 cells/well and incubated overnight under standard cultivation conditions. Next day, medium was aspirated, and cells incubated in RPMI + 1% FCS medium with 50 and 100 ng/ml BMP-4, 5 µM LDN-214117 or vehicle. Cell growth, i.e., confluence of the cells in each well was monitored every 6 h for 5 days. Bright field images were acquired and analyzed via IncuCyte® S3 Software (Essen Bioscience Inc., Ann Arbor, MI, USA).

Scratch-wound healing assay

To examine the ability of LCLC-103H cells for wound closure under different treatment conditions, IncuCyte® Scratch Wound Assay (Essen Bioscience) was performed following manufacturer's instructions. Briefly, cells were seeded in an assay-specific 96 Well ImageLock Microplate in high density (2.5×10^4 cells/well) in cultivation medium and left overnight to adhere. Then, in order to reduce cell proliferation, medium was changed to serum-free RPMI, and cells were incubated for another 48 h. After serum starvation, wound area in each well was formed using IncuCyte® WoundMaker tool (Essen Bioscience), cells washed twice and incubated in RPMI + 1% FCS medium with 50 and 100 ng/ml BMP-4, 5 µM LDN-214117 or vehicle. Migration of LCLC-103H cells into the wound area was monitored every 3 h for 72 h and collected images were analyzed via IncuCyte® Scratch Wound Cell Migration Software Module (Essen Bioscience).

Trans-well migration assay

3×10^5 LCLC-103H cells were seeded in RPMI+10% FCS medium in 8-µm-pore-sized trans-well inserts—ThinCerts™ Inserts, 6 well (Greiner Bio-One). The inserts were then placed on the 6-well cell culture plate filled with RPMI+10% FCS medium and left overnight to settle down. Next day, medium above the cells was replaced with serum-free RPMI medium and inserts transferred onto the 6-well cell culture plate containing 3 ml/well of appropriate RPMI medium—serum-free for chemotaxis negative control, supplemented with 10% FCS for chemotaxis positive control, and serum-free containing 100 ng/ml BMP-4 or 5 µM LDN-214117 as test. Inserts were incubated for 24 h at 37 °C and 5% CO_2. Cells that migrated through the pores to the membrane's outer side were stained with DiffQuick® Staining set (Medion Diagnostics GmbH, Düdingen, Germany) and

embedded on microscope slides. Five bright field images per membrane were taken on the Axiovert 25 inverted microscope (Carl Zeiss Microscopy GmbH, Jena, Germany) under 100× magnification. Cells were counted manually using ImageJ 1.50e software (Schneider et al. 2012).

Multicellular spheroid formation

LCLC-103H cells were grown to 90% confluence and dissociated with Trypsin-EDTA (0.05%) (Thermo Fisher Scientific). 5000 cells per well were seeded into a 96-well u-bottomed Greiner microwell plate (Greiner Bio-One) and centrifuged at 200 rcf for 5 min to allow the cells to sediment at the bottom of the well. Incubation was performed for 4 days in a humidified atmosphere at 37 °C, 5% CO_2. Spheroid formation was performed and monitored in an IncuCyte™ ZOOM live cell analyzer (Essen Bioscience).

Treatment of multicellular spheroids with BMP-4 and LDN-214117

On day 4, the medium of the spheroids was removed and the spheroids were immediately washed with PBS (Thermo Fisher Scientific). Afterwards the agents for incubation were prepared in fresh RPMI medium supplemented with GlutaMAX™ without phenol red (Thermo Fisher Scientific) and 1% FCS as followed: 50 ng/mL BMP-4, 100 ng/mL BMP-4, 5 µM LDN-214117, 50 ng/mL BMP-4 + 5 µM LDN-214117. Controls were prepared with 1% and 10% FCS (Biochrom), respectively.

RT-qPCR

Gene expression analysis included seeding LCLC-103H cells in T25 cell culture flasks in cultivation medium and a concentration of 2×10^5 cells/flask. After overnight incubation and a 12–16-hour serum deprivation, treatment of the cells with BMP-4, LDN-214117 or vehicle in RPMI + 1% FCS medium was performed. Cells were harvested using plastic cell scraper 24, 48 and 72 h after the treatment. RNA isolation of harvested cells was done using InnuPREP RNA Mini Kit (Analytik Jena AG, Jena, Germany) following manufacturer's instructions. Concentration and quality of isolated RNA were determined on NanoDrop™ 2000 Spectrophotometer (PEQLAB Biotechnology GmbH, Erlangen, Germany). cDNA synthesis was performed using Moloney Murine Leukemia Virus Reverse Transcriptase (M-MLV RT, Invitrogen, Carlsbad, CA, USA) on thermocycler Mastercycler® gradient (Eppendorf AG, Hamburg, Germany). Quantitative real-time PCR (qPCR) based on the SYBR-Green I DNA-binding technology was used for detection and quantification of specific cDNA sequences. Target-specific primers were applied (see Supplement Table S2).

Statistical analysis

Data analysis was performed via GraphPad PRISM® software, version 6.01 (GraphPad Software Inc., La Jolla, CA, USA). One-way analysis of variance (ANOVA) with 95% confidence interval was applied, followed by a multiple comparison test and correction according to Dunnett and Tukey. Spheroid sizes were determined with ImageJ (Schneider et al. 2012) and analyzed with SPSS statistics software, version 21 (IBM Inc., Armonk, NY, USA) using one-way ANOVA followed by Tukey test. Differences are considered as statistically significant for $p < 0.05$.

Results

Canonical BMP signaling pathway is active in LCLC-103H lung cancer cells

BMP-4 treatment of LCLC-103H lung cancer cells triggered the activation of canonical SMAD-dependent BMP signaling. This was confirmed by the detection of a strong increase in phosphorylated form of SMAD1, 5 and 9 (pSMAD1/5/9) as early as 30 min after the treatment (Fig. 1a, b). Using Western blot analysis, we were able to detect the phosphorylation event with 50 ng/ml and 100 ng/ml, but not with 2 ng/ml BMP-4 concentration. The increase in the amount of pSMAD1/5/9 stayed significant even 24 h after the treatment, compared to the vehicle control cells. The activation of SMAD-dependent signaling was successfully blocked by BMP receptor type I antagonist, LDN-214117, when used alone or as a pre-treatment before BMP-4 stimulation.

The ability of BMP-4 to activate and that of LDN-214117 to block SMAD-dependent BMP signaling was also observed on *ID1*, a BMP target gene. We showed a steady increase of ID1 protein starting from 30 min up to 3 and 24 h after stimulation of the investigated lung cancer cell line with 50 and 100 ng/ml BMP-4 (Fig. 1a, c). The effect was completely diminished 3 h after LDN-214117 incubation of LCLC-103H cells. A 30-min pre-treatment with LDN-214117 before BMP-4 incubation was not as efficient in blocking ID1 production, suggesting a time-dependent effect of LDN-214117 activity on gene regulation level and/or a BMP signaling pathway other than SMAD-dependent that is responsible for *ID1* targeting.

Inhibition of BMP signaling causes apoptosis of LCLC-103H cells and reduces their proliferation

Influence of BMP signaling on viability of LCLC-103H cells was investigated via flow cytometric assay employing Annexin-V (AnnV) and propidium iodide (PI). The inhibition of BMP signaling by LDN-214117 treatment

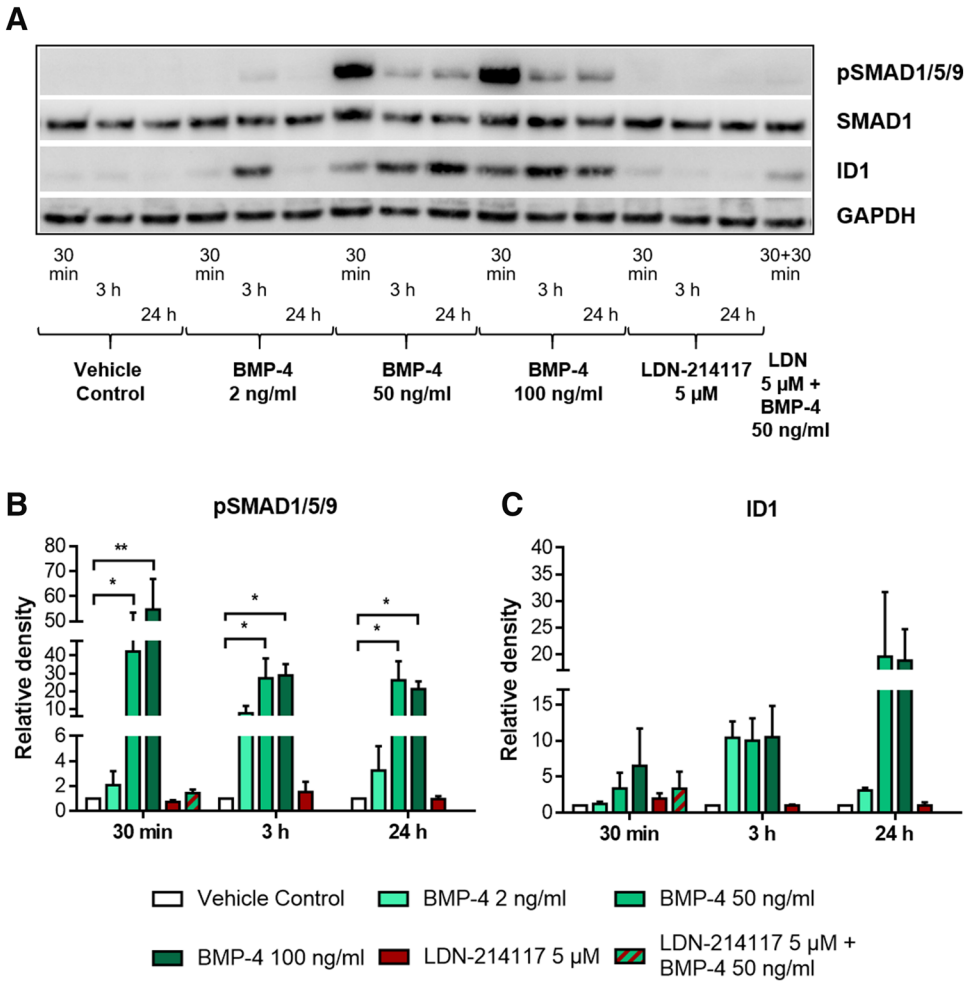

Fig. 1 BMP-4 activates SMAD-dependent BMP signaling pathway in LCLC-103H cells via phosphorylation of SMAD1/5/9. **a** Western blot detection of SMAD1/5/9 phosphorylation and ID1 after BMP-4 and LDN-214117 treatment of LCLC-103H cells at various time points, as depicted on the representative blot. **b** Semi-quantitative analysis of pSMAD1/5/9, relative to total SMAD1 and GAPDH, respectively, performed using ImageJ ($n=3$). Data are shown as mean ± SEM. $*p<0.05$, $**p<0.01$, as determined by one-way ANOVA with Dunnett's multiple comparison test, and 95% confidence interval. **c** Semi-quantitative analysis of ID1, relative to GAPDH, respectively, performed using ImageJ ($n=3$). LDN—LDN-214117; LDN 5 µM + BMP-4 50 ng/ml—first treatment with LDN-214117 for 30 min, then 30-min treatment with BMP-4

reduced the cell viability in a time-dependent manner. A strong decrease in the viable $AnnV^-/PI^-$ population of LDN-214117-treated cells was first observed 72 h after the treatment. The cell viability under LDN-214117 treatment decreased markedly with time, counting approximately 60% of the vehicle control level at the 96-h measurement point. The viability of LCLC-103H cells was not affected by BMP-4 in any of the concentrations used and remained on the control level after the treatment (Fig. 2a, b).

Further analysis revealed that LDN-214117 treatment induced considerable death of LCLC-103H cells: it led to a threefold and fivefold increase in early-apoptotic events, compared to the control, 3 and 4 days after the treatment, respectively; it resulted also in a twofold increase in late-apoptotic and necrotic cell-subpopulation, compared to the control group, which was observed as soon as 2 days after the incubation (Fig. 2b). Importantly, cells under BMP-4 treatment did not undergo apoptosis in higher rate than those in the control group, with a tendency to react even with a reduced level of apoptotic and necrotic events at later time points.

Growth of LCLC-103H cells after incubation with BMP-4 or LDN-214117 was evaluated via cell confluence assay using the IncuCyte® live cell imaging system (Essen Bioscience) (Fig. 2c). Under normal cultivation conditions, in RPMI+10% FCS medium, LCLC-103H cells reached confluence of more than 90% in 72 h, with an exponential increase in cell density between 24 h and 48 h after seeding (Figs. 2c, S1). This pattern of growth kinetics was rather changed in serum-deprived conditions (RPMI + 1% FCS) under the treatment of LCLC-103H cells with BMP-4, LDN-214117 or vehicle. Confluence of LCLC-103H cells treated with LDN-214117 differed significantly compared to other treatment groups, showing maximum of only 70% cell density within 5 days of cultivation. Although without the phase of sharp increase in cell density observed in RPMI+10% FCS conditions, the BMP-4-treated and vehicle control cell cultures were still able to reach confluence of over 90% after 96 h. Additionally, there was no difference in cell confluence rate between the BMP-4 and vehicle control cell cultures.

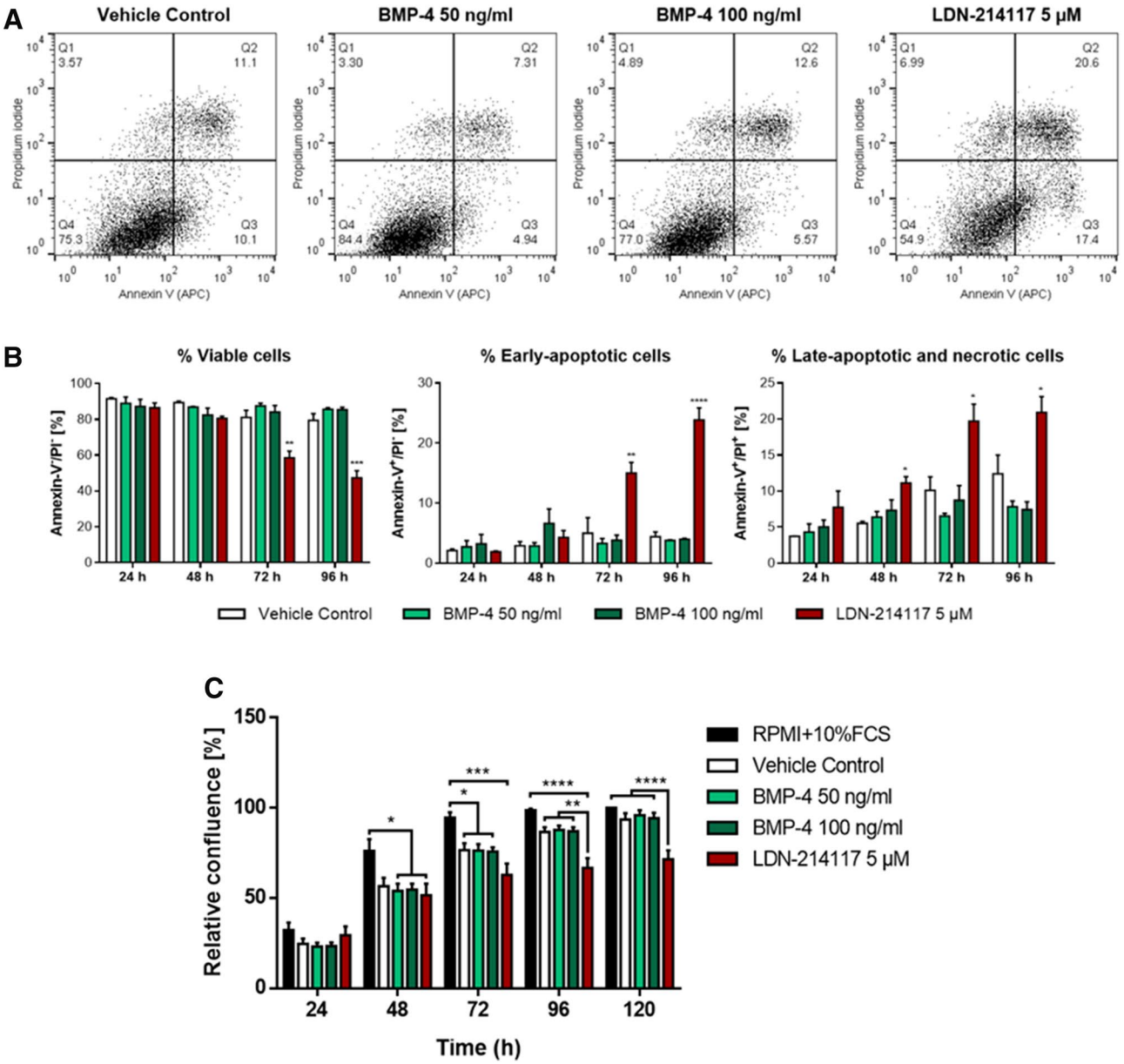

Fig. 2 BMP receptor type I inhibition via LDN-214117 reduces viability and proliferation of lung carcinoma cells LCLC-103H. **a** Representative dot plots of flow cytometric cell viability measurement on LCLC-103H cells 72 h under different treatments, as depicted. **b** Viable, early-apoptotic, and late-apoptotic and necrotic cell-like events every 24 h within 4 days after indicated treatments on LCLC-103H cells ($n=3$). **c** Monitoring of confluence rate of LCLC-103H cells under different cultivation conditions within 5 days via IncuCyte® live cell imaging system ($n=5$). Data are plotted as mean ± SEM. $*p<0.05$, $**p<0.01$, $***p<0.001$, $****p<0.0001$, as determined by one-way ANOVA with **b** Dunnett's and **c** Tukey's multiple comparison test, and 95% confidence interval

BMP signaling is necessary for migration of LCLC-103H cells

After proving that LCLC-103H cells respond to BMP-4 stimulation without major consequences for their viability and growth rate, functional studies were conducted to investigate the influence of the BMP signaling on migration of LCLC-103H cells.

Wound healing assay was performed using the IncuCyte® system (Essen Bioscience). The migration of LCLC-103H cells into the wound area under different medium conditions was monitored in real time for a total of 48 h (Fig. 3a). The representative images show that LCLC-103H cells in RPMI+10% FCS medium were capable of closing the wound in approximately 48 h. The ability of LCLC-103H cells to migrate into the wound

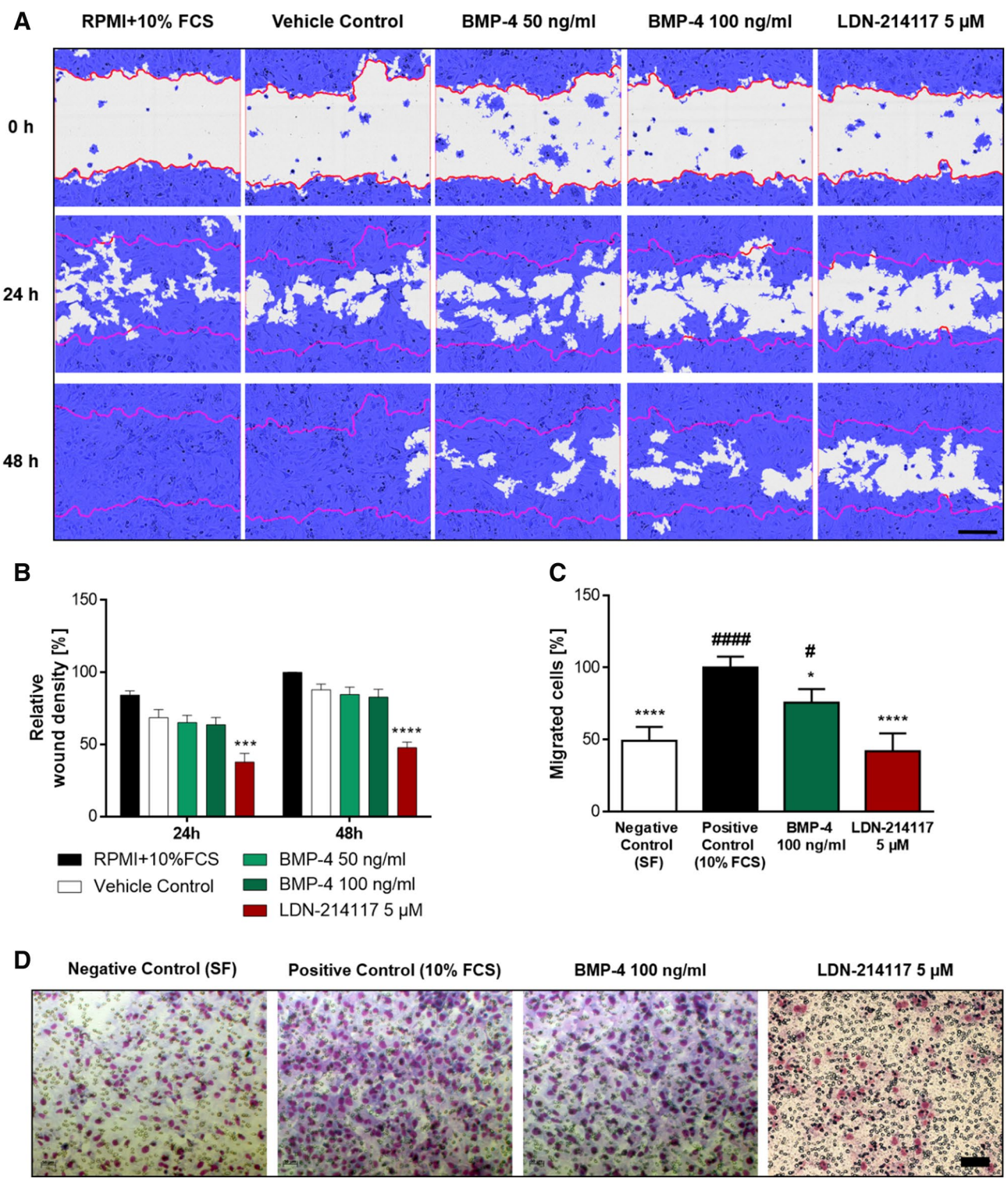

Fig. 3 BMP receptor type I inhibition by LDN-214117 suppresses wound healing and chemotactic potential of LCLC-103H cells. **a** IncuCyte® monitoring of scratch-wound healing by LCLC-103H cells under different medium conditions. **b** Recorded bright field images are analyzed for the cell confluency in the initial wound area (red line) determined at "zero" time point ($n=3$). **c** Enumeration of migrated cells performed using ImageJ software and percent of migrated cells calculated relative to positive control ($n=4$). **d** Representative bright field images of migrated LCLC-103H cells in transwell insert system. Data are plotted as mean **b** ±SEM and **c** ±SD. *$p<0.01$, ****$p<0.0001$, as determined by one-way ANOVA with **b** Dunett's and **c** Tukey's multiple comparison test, and 95% confidence interval. *Compared to the positive control (RPMI + 10% FCS), #Compared to the negative control (SF RPMI). Scale bar **a** 300 µm, **d** 100 µm. Magnification 100×. *SF* serum free

area was considerably impaired under LDN-214117 treatment, resulting in an incomplete wound closure at the end time point ($t = 48$ h). Wound density analysis (Fig. 3b) led to the similar conclusion. Inhibition of BMP signaling via LDN-214117 significantly hindered the migration of LCLC-103H cells into the wound area, reaching relative wound density of only 50% in 48 h. Wound closure potential of LCLC-103H cells with stimulated BMP signaling was maintained on the vehicle control level, regardless of the dose of BMP-4 applied.

Using trans-well insert system, the potential of BMP-4 to act as chemoattractant for migration of LCLC-103H cells was further investigated. LCLC-103H cells showed enhancement of 25% in chemotaxis-induced motility in the presence of BMP-4 concentration gradient compared to the negative control. Also, BMP-4 as chemoattractant in serum-free medium induced the cells to trans-migrate in the number as high as 75% of the number of migrated cells in the presence of serum (positive control, 10% FCS) as chemoattractant. LDN-214117 led to more than 50% decrease in chemotactic motility of LCLC-103H cells compared to the serum-induced chemotaxis, keeping the percent of migrated cells on the level of negative control (Fig. 3c).

Activation of BMP signaling supports the growth of LCLC-103H cells

To get closer to in vivo conditions, we established multicellular spheroid cell cultures from LCLC-103H cells. After 4 days of cultivation, the spheroids reached a medium diameter of 300–400 µm. They were incubated with BMP-4 (50 and 100 ng/ml), LDN-214117 (5 µM) and a combination of BMP-4 (50 ng/ml) and LDN-214117 (5 µM) under serum-reduced conditions (RPMI + 1% FCS). The spheroids were monitored with the IncuCyte system and documented continuously. The size of the spheroids after 48 h of incubation was determined and compared to the initial size (time point 0 h). The control group supplemented with RPMI+10% FCS showed an almost 30% increase in size (129% ± 24% SD). The BMP-4 incubated spheroids reached 117% ± 13% SD of the initial size independent of the BMP-4 concentration. In contrast, the LDN-214117 treated multicellular spheroids achieve only an increase of 6% (106 ± 11% SD). This value was even less than the spheroids cultivated with

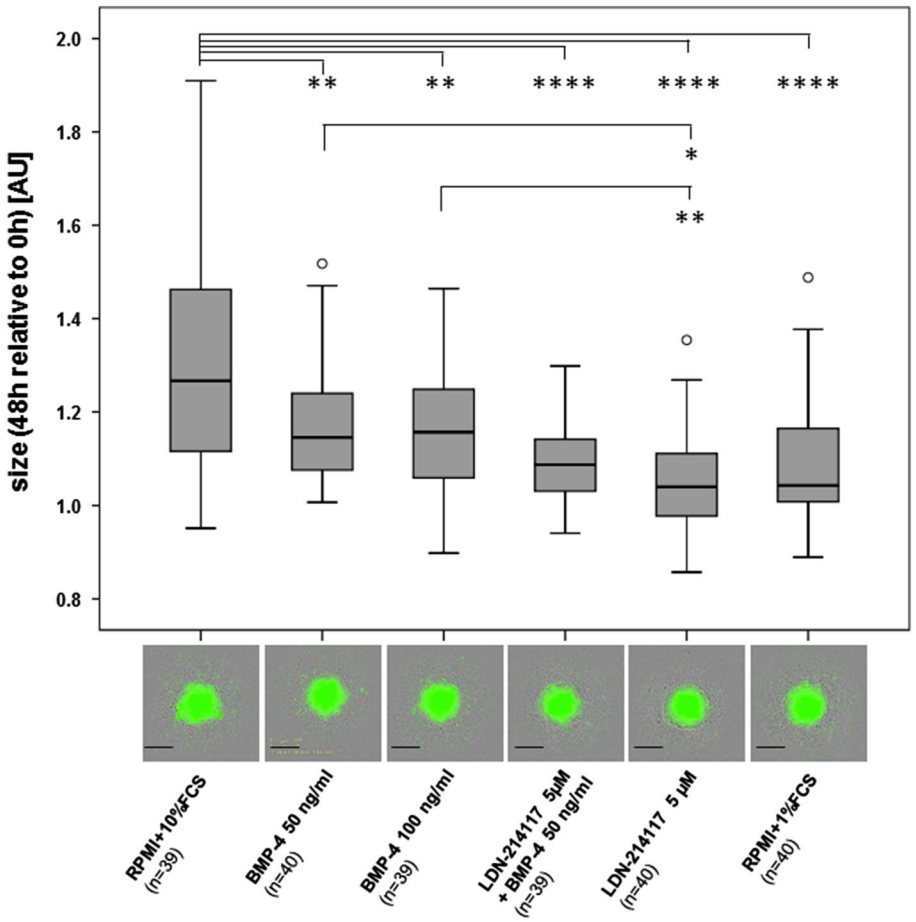

Fig. 4 BMP receptor type I inhibition by LDN-214117 hinders growth of multicellular LCLC-103H spheroids. 4 days after seeding spheroids with a diameter of 300–400 µm were incubated with different medium conditions. The size of the spheroids was measured at the start of the incubation and after 48 h using ImageJ software. The ratio size48h:size0h is presented. $*p < 0.05$, $**p < 0.01$, $****p < 0.0001$ as determined by Mann–Whitney test and 95% confidence interval. Representative images of incubated spheroids are shown below the boxplot (scale bar 300 µm). $n = 39/40$

serum-reduced medium (108% ± 13% SD) and the LCLC-103H spheroids treated with the combination of 50 ng/ml BMP-4 and 5 µM LDN-214117 (109% ± 9% SD) (Fig. 4).

BMP signaling is involved in epithelial–mesenchymal transition in LCLC-103H cells

Observed changes in migratory potential of LCLC-103H cells via modulation of BMP signaling were further investigated at the molecular level. Here, the capacity of BMP-4 to induce epithelial–mesenchymal transition (EMT) was examined as a potential basis for its influence on migratory properties of investigated cells. Gene expression analysis of several EMT markers, such as Snail and Slug, as well as of S100A4 was performed.

Activation of BMP signaling in LCLC-103H cells resulted in a sharp and consistent increase in mRNA level of the EMT transcription factors (EMT-TFs) Slug and Snail. The relative expression ratio of Slug and Snail showed two and threefold change, respectively, after BMP-4 treatment. The effect remained constant within 3 days after the treatment. Inhibition of the BMP signaling by LDN-214117 induced distinct gene expression patterns for the two EMT-TFs. While LDN-214117 led to the significant down-regulation of Snail at all time points after the treatment, it kept Slug mRNA on the control level after transiently increasing it 24 h after the treatment (Fig. 5).

LCLC-103H cells under BMP-4 treatment expressed significantly higher ratio of S100A4 mRNA, showing an average 1.6-fold change compared to the control cells 24, 48 and 72 h after the treatment. Depending on the time point observed, incubation with LDN-214117 resulted in the opposite, but less pronounced effect, or in no change in S100A4 mRNA levels compared to the control group.

Discussion

In this study, we demonstrate that BMP signaling plays a critical role in viability and migration of non-small cell lung carcinoma cell line LCLC-103H. We show that the cells respond to BMP-4 via canonical BMP signaling, as proved by detection of SMAD1/5/9 phosphorylation and inhibition of the effect via LDN-214117. The BMP signaling in LCLC-103H cells appears to be essential for maintenance of cell viability and growth. Inhibition of the signaling by LDN-214117 results in lung cancer cell apoptosis and reduced cell proliferation. Also, blocking BMP signaling by LDN-214117 suppresses chemotactic motility and wound healing ability of LCLC-103H cells. The underlying mechanism for hindered cell migration under LDN-214117 treatment involves down-regulation of EMT transcription factors, especially Snail. Altogether, the data suggest that BMP signaling might be considered a potential novel therapeutic target in the treatment of non-small cell lung carcinoma.

BMP-4 activates canonical SMAD-dependent signaling in LCLC-103H cells. The canonical BMP pathway includes the activation of BMP receptors type I and II after ligand

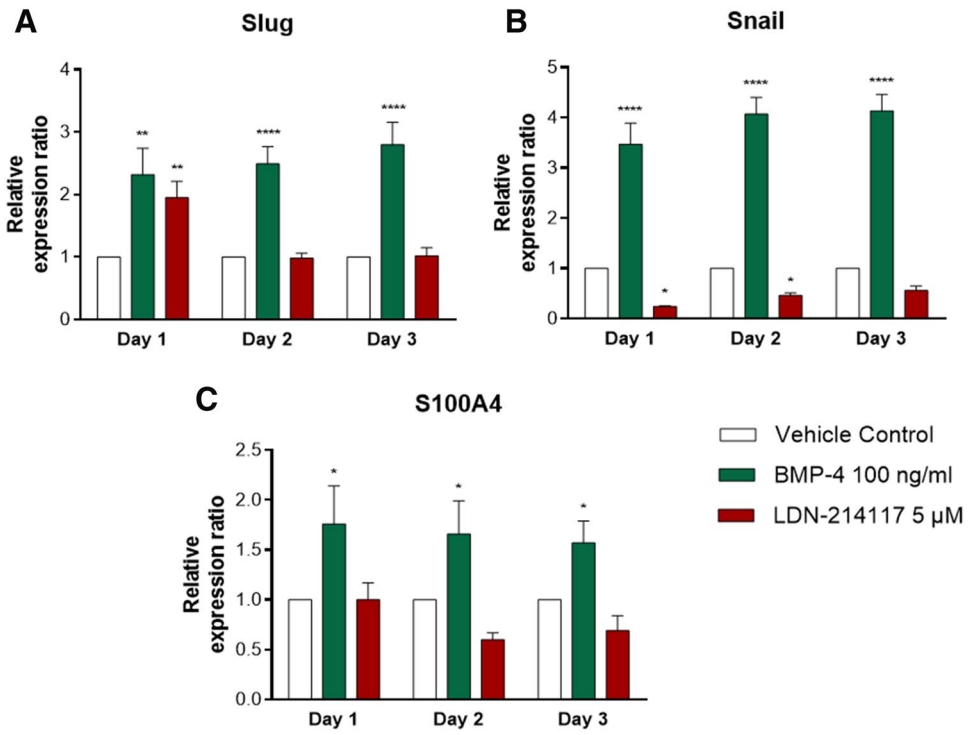

Fig. 5 BMP-4 induces epithelial–mesenchymal transition in LCLC-103H cells. Relative expression ratio for **a** Slug, **b** Snail, and **c** S100A4 in LCLC-103H cells after treatment with BMP-4, LDN-214117 or control ($n = 3$). Data are shown as mean ± SD. *$p < 0.05$, **$p < 0.01$, ****$p < 0.0001$, as determined by one-way ANOVA with Dunnett's multiple comparison test, and 95% confidence interval

binding, which is followed by substantial phosphorylation of SMADs [SMAD1, 5, and 8 (or its splicing variant, SMAD9)]. The phosphorylated SMADs translocate into the nucleus to regulate gene expression (Miyazono et al. 2005). On LCLC-103H cells, we show that phosphorylated SMAD1/5/9 is significantly increased shortly after BMP-4 treatment and remains elevated at least 24 h after the treatment. In contrast, the BMP receptor type I antagonist LDN-214117 efficiently blocks the BMP-4-induced phosphorylation of SMAD1/5/9. This proves that LCLC-103H cells possess functional SMAD-dependent BMP signaling machinery, which can be successfully inhibited using LDN-214117. The finding is reported commonly on lung adenocarcinoma cell lines using BMP-2 and small molecule BMP receptor type I antagonists (Fotinos et al. 2014; Langenfeld et al. 2013). The effect of BMP-4 on LCLC-103H cells is not accompanied by the activation of other non-canonical SMAD-independent signaling pathways, such as PI3K/AKT, p38 and ERK MAPK (data not shown). However, inhibition of BMP signaling via LDN-214117 treatment leads to increased phosphorylation of ERK1/2 (data shown in the Supplement, Fig. S2). Since no opposite effect on the ERK MAPK pathway under BMP-4 treatment was observed, the result might reflect an off-target effect of LDN-214117. However, an antagonistic relation between canonical BMP-4 signaling and ERK MAPK pathway has been described earlier, as in the case of cell-fate decision mechanisms in *Xenopus* ectoderm (Goswami et al. 2001), in self-renewal of murine embryonic stem cells (Qi et al. 2004; Zhang and Li 2005), and in mink lung epithelial cells (Kretzschmar et al. 1997).

Protein analysis was used to examine changes in ID1 level, a down-stream target of BMP signaling, after BMP-4 treatment. ID1 is an early gene-response protein of the BMP signaling and the protein amount is expected to increase within first 2 hours after BMP stimulation (Hollnagel et al. 1999; Miyazono and Miyazawa 2002). BMP-4-induced activation of SMAD-dependent BMP signaling in LCLC-103H cells is further followed by the increase in ID1 protein levels. The effect is time dependent in the case of both BMP-4 and LDN-214117, with the effects becoming clearly detectable 3 h after indicated treatments. The finding is in corroboration with previous reports, confirming ID1 as an early gene-response protein of the BMP signaling in investigated cells (Miyazono and Miyazawa 2002).

BMP signaling is important for the viability and growth of LCLC-103H cells. The inhibition of BMP signaling via LDN-214117 leads to a significant reduction of viable LCLC-103H cell population, triggering cell apoptosis and necrosis within 48 h. Viability of the cells after BMP-4 treatment is not negatively affected compared to the vehicle control, and the effect is maintained even 4 days after the treatment in low-serum conditions. Comparably, cultivation of LCLC-103H cells with BMP-4 did not show a change in confluence rate from that of the vehicle control cells, while LDN-214117-treated cells exhibited drastically lower growth rate and were not able to reach more than 75% confluence of vehicle control cells until the end of the monitoring period (5 days). The previously mentioned investigations were performed in 2D cell culture. For the sake of bridging the gap between in vitro and in vivo conditions, multicellular spheroid culture models were established (Müller-Klieser 1987). These 3-dimensional cell aggregates exhibit a strong comparability with solid tumors regarding cell–cell and cell–matrix interactions and are frequently used as pharmacological models for efficacy testing of therapeutics (Hirschhaeuser et al. 2010). To monitor the effects of growth regulating factors, phase-contrast imaging is used. The delay of spheroidal growth is a classical endpoint using the difference between treated and untreated spheroids (Friedrich et al. 2009). LDN-214117-treated spheroids behave as spheroids under serum-reduced conditions, whereas BMP-4 addition allows a moderate growth of the spheroids. The findings are in corroboration with reports on suppression of cell growth and proliferation as well as of apoptosis and necrosis induction after BMP receptor type I signaling inhibition—in colorectal carcinoma cells (Yokoyama et al. 2017), and lung adenocarcinoma cells (Fotinos et al. 2014; Hao et al. 2014; Langenfeld et al. 2013).

BMP signaling is important for chemotactic and wound healing migratory properties of LCLC-103H cells. BMP-4 acts as chemoattractant for LCLC-103H cells, increasing the number of migrated cells in trans-well system for approximately 50% compared to the negative control level. Also, BMP-4 alone leads to the amount of migrated cell reaching 75% of that in the case of medium with 10% FCS (positive control) as chemoattractant. In the same assay, LDN-214117 abrogates the ability of the LCLC-103H cells to trans-migrate, keeping the number of migrated cells on the level of negative control. In the wound healing assay, the BMP-4 treatment sustains the motility of LCLC-103H cells on the vehicle control level, while the inhibition of BMP signaling via LDN-214117 significantly hinders the ability of the cells to close the scratch wound. BMP-4-mediated enhancement of migration and invasion properties is described in the context of pancreatic (Virtanen et al. 2011), breast (Ampuja et al. 2013; Park et al. 2015), hepatocellular (Zeng et al. 2017), squamous-cell carcinoma of head and neck (Xu et al. 2011), as well as in human embryonic stem cells (Richter et al. 2014), and normal airway epithelial cells (McCormack et al. 2013). Inhibition of BMP signaling with a consequent suppression of growth, motility and invasiveness is elaborated on a wide range of lung adenocarcinoma (Hao et al. 2014; Kim et al. 2015; Langenfeld et al. 2013; Ye et al. 2012),

and one large cell lung carcinoma cell line H460 (Hao et al. 2014), as well as on breast carcinoma cell lines (Pickup et al. 2015).

The increase in the cell motility after BMP-4 treatment is commonly regarded to be the result of EMT induction in the investigated cell lines (Gonzalez and Medici 2014; McCormack et al. 2013; Park et al. 2015; Zeng et al. 2017; Zhang et al. 2016). Therefore, the next step in examining BMP-4-driven chemotaxis of LCLC-103H cells was deciphering possible underlying molecular mechanisms with a focus on EMT initiation in the cell line. After BMP signaling activation, LCLC-103H cells enter EMT through considerable up-regulation of EMT transcription factors, Snail and Slug, and that of mesenchymal marker, S100A4. The up-regulation of Snail, Slug and S100A4 is accompanied by a short-term dysregulation of vimentin and E-cadherin, increase and decrease, respectively (data not shown). The inhibition of BMP signaling via LDN-214117 consistently induces opposite effects on the mRNA level compared to that of BMP-4. The most pronounced effect of LDN-214117 was observed on Snail mRNA levels, which appeared significantly down-regulated at least 72 h after the treatment, compared to the control level. The results propose Snail as an essential EMT TF in the BMP signaling-mediated regulation of LCLC-103H migration potential.

The results demonstrated in this work provide evidence for pro-migratory and pro-EMT activity of BMP-4 on the LCLC-103H cells through BMP receptor type I SMAD-dependent signaling. The findings raise the possibility of considering BMP signaling inhibition as a novel therapeutic tool for non-small cell lung carcinoma treatment. Nevertheless, further studies with a deeper insight into the proteomics, epigenetics and genetics of a wider spectrum of lung cancer cell lines and tissue specimens are necessary for the evaluation and validation of a BMP receptor-related therapeutic approach.

Acknowledgements The technical assistance of Cornelia Jörke is greatly acknowledged. We highly appreciate Dr. Mike Fischer for helpful instructions with flow cytometry and Dr. Katrin Hoffmann for support with statistical analysis. We also would like to thank Dr. Christine Gräfe for her helpful support in preparing and paraphrasing this manuscript. JM received a scholarship from the Interdisziplinäres Zentrum für Klinische Forschung (IZKF) Jena. This work was supported in part by Europäische Fonds für regionale Entwicklung-Europa für Thüringen (EFRE, FKZ 2016 FGI 0006).

Compliance with ethical standards

Conflict of interest All authors declare that they have no conflict of interest.

Human and animal participants This article does not contain any studies with human participants or animals performed by any of the authors.

References

Alarmo EL, Kallioniemi A (2010) Bone morphogenetic proteins in breast cancer: dual role in tumourigenesis? Endocr Relat Cancer 17:R123–R139

Alarmo EL, Huhtala H, Korhonen T, Pylkkänen L, Holli K, Kuukasjärvi T, Parkkila S, Kallioniemi A (2013) Bone morphogenetic protein 4 expression in multiple normal and tumor tissues reveals its importance beyond development. Mod Pathol 26:10–21

Ampuja M, Jokimäki R, Juuti-Uusitalo K, Rodriguez-Martinez A, Alarmo EL, Kallioniemi A (2013) BMP4 inhibits the proliferation of breast cancer cells and induces an MMP-dependent migratory phenotype in MDA-MB-231 cells in 3D environment. BMC Cancer 13:429–442

Ampuja M, Alarmo EL, Owens P, Havunen R, Gorska AE, Moses HL, Kallioniemi A (2016) The impact of bone morphogenetic protein 4 (BMP4) on breast cancer metastasis in a mouse xenograft model. Cancer Lett 375:238–244

Bellusci S, Henderson R, Winnier G, Oikawa T, Hogan BL (1996) Evidence from normal expression and targeted misexpression that bone morphogenetic protein (Bmp-4) plays a role in mouse embryonic lung morphogenesis. Development 122:1693–1702

Bénazet JD, Bischofberger M, Tiecke E, Gonçalves A, Martin JF, Zuniga A, Naef F, Zeller R (2009) A self-regulatory system of interlinked signaling feedback loops controls mouse limb patterning. Science 323:1050–1053

Bepler G, Koehler A, Kiefer P, Havemann K, Beisenherz K, Jaques G, Gropp C, Haeder M (1988) Characterization of the state of differentiation of six newly established human non-small-cell lung cancer cell lines. Differentiation 37:158–171

Brandao GDA, Brega EF, Spatz A (2012) The role of molecular pathology in non-small-cell lung carcinoma-now and in the future. Curr Oncol 19:S24–S832

Buckley S, Shi W, Driscoll B, Ferrario A, Anderson K, Warburton D (2004) BMP4 signaling induces senescence and modulates the oncogenic phenotype of A549 lung adenocarcinoma cells. Am J Physiol Lung Cell Mol Physiol 286:L81–L86

Clement JH, Marr N, Meissner A, Schwalbe M, Sebald W, Kliche KO, Höffken K, Wölfl S (2000) BMP-2 induces sequential changes of ID gene expression in the breast cancer cell line MCF-7. J Cancer Res Clin Oncol 126:271–279

Danesh SM, Villasenor A, Chong D, Soukup C, Cleaver O (2009) BMP and BMP receptor expression during murine organogenesis. Gene Expr Patterns 9:255–265

Deng H, Ravikumar TSS, Yang WL (2009) Overexpression of bone morphogenetic protein 4 enhances the invasiveness of Smad4-deficient human colorectal cancer cells. Cancer Lett 281:220–231

Fang WT, Fan CC, Li SM et al (2014) Downregulation of a putative tumor suppressor BMP4 by SOX2 promotes growth of lung squamous cell carcinoma. Int J Cancer 135:809–819

Ferlay J, Soerjomataram I, Dikshit R, Eser S, Mathers C, Rebelo M, Parkin DM, Forman D, Bray F (2015) Cancer incidence and mortality worldwide: sources, methods and major patterns in GLOBOCAN 2012. Int J Cancer 136:E359–E386

Ferlay J, Ervik M, Lam F, Colombet M, Mery L, Piñeros M, Znaor A, Soerjomataram I, Bray F (2018). Global cancer observatory: cancer today. International Agency for Research on Cancer, Lyon. https://gco.iarc.fr/today. Accessed 14 Feb 2019

Fotinos A, Nagarajan N, Martins AS, Fritz DT, Garsetti D, Lee AT, Hong CC, Rogers MB (2014) Bone morphogenetic protein-focused strategies to induce cytotoxicity in lung cancer cells. Anticancer Res 34:2095–2104

Friedrich J, Seidel C, Ebner R, Kunz-Schughart LA (2009) Spheroid-based drug screen: considerations and practical approach. Nature Protoc 4:309–324

Gonzalez DM, Medici D (2014) Signaling mechanisms of the epithelial-mesenchymal transition. Sci Signal 7(344):re8. https://doi.org/10.1126/scisignal.2005189

Goswami M, Uzgare AR, Sater AK (2001) Regulation of MAP kinase by the BMP-4/TAK1 pathway in Xenopus ectoderm. Dev Biol 236:259–270

Guo D, Huang J, Gong J (2012) Bone morphogenetic protein 4 (BMP4) is required for migration and invasion of breast cancer. Mol Cell Biochem 363:179–190

Hao J, Lee R, Chang A, Fan J, Labib C, Parsa C, Orlando R, Andresen B, Huang Y (2014) DMH1, a small molecule inhibitor of BMP type I receptors, suppresses growth and invasion of lung cancer. PLoS One 9:e90748. https://doi.org/10.1371/journal.pone.0090748

Haramis APG, Begthel H, van den Born M, van Es J, Jonkheer S, Offerhaus GJA, Clevers H (2004) De novo crypt formation and juvenile polyposis on BMP inhibition in mouse intestine. Science 303:1684–1686

Haubold M, Weise A, Stephan H, Dünker N (2010) Bone morphogenetic protein 4 (BMP4) signaling in retinoblastoma cells. Int J Biol Sci 6:700–715

Hirschhaeuser F, Menne H, Dittfeld C, West J, Mueller-Klieser W, Kunz-Schughart LA (2010) Multicellular tumor spheroids: an underestimated tool is catching up again. J Biotechnol 148:3–15

Hollnagel A, Oehlmann V, Heymer J, Rüther U, Nordheim A (1999) Id genes are direct targets of bone morphogenetic protein induction in embryonic stem cells. J Biol Chem 274:19838–19845

Kallioniemi A (2012) Bone morphogenetic protein 4-a fascinating regulator of cancer cell behavior. Cancer Genet 205:267–277

Kim JS, Kurie JM, Ahn YH (2015) BMP4 depletion by miR-200 inhibits tumorigenesis and metastasis of lung adenocarcinoma cells. Mol Cancer 14:173–183

Kretzschmar M, Doody J, Massagué J (1997) Opposing BMP and EGF signalling pathways converge on the TGF-beta family mediator Smad1. Nature 389:618–622

Langenfeld E, Hong CC, Lanke G, Langenfeld J (2013) Bone morphogenetic protein type I receptor antagonists decrease growth and induce cell death of lung cancer cell lines. PLoS One 8:e61256. https://doi.org/10.1371/journal.pone.0061256

Lubbe SJ, Pittman AM, Olver B, Lloyd A, Vijayakrishnan J, Naranjo S, Dobbins S, Broderick P, Gómez-Skarmeta JL, Houlston RS (2012) The 14q22.2 colorectal cancer variant rs4444235 shows cis-acting regulation of BMP4. Oncogene 31:3777–3784

Maegdefrau U, Amann T, Winklmeier A et al (2009) Bone morphogenetic protein 4 is induced in hepatocellular carcinoma by hypoxia and promotes tumour progression. J Pathol 218:520–529

McCormack N, Molloy EL, O'Dea S (2013) Bone morphogenetic proteins enhance an epithelial-mesenchymal transition in normal airway epithelial cells during restitution of a disrupted epithelium. Respir Res 14:36. https://doi.org/10.1186/1465-9921-14-36

Miyazaki Y, Oshima K, Fogo A, Ichikawa I (2003) Evidence that bone morphogenetic protein 4 has multiple biological functions during kidney and urinary tract development. Kidney Int 63:835–844

Miyazono K, Miyazawa K (2002) Id: a target of BMP signaling. Science's STKE 2002(151):pe40. https://doi.org/10.1126/stke.2002.151.pe40

Miyazono K, Maeda S, Imamura T (2005) BMP receptor signaling: transcriptional targets, regulation of signals, and signaling cross-talk. Cytokine Growth Factor Rev 16:251–263

Miyazono K, Kamiya Y, Morikawa M (2010) Bone morphogenetic protein receptors and signal transduction. J Biochem 147:35–51

Müller P, Doliva R, Busch M, Philippeit C, Stephan H, Dünker N, Makishima M (2015) Additive effects of retinoic acid (RA) and bone morphogenetic protein 4 (BMP-4) apoptosis signaling in retinoblastoma cell lines. PLoS One 10:1–22

Müller-Klieser W (1987) Multicellular spheroids. A review on cellular aggregates in cancer research. J Cancer Res Clin Oncol 113:101–122

Park KS, Dubon MJ, Gumbiner BM (2015) N-cadherin mediates the migration of MCF-10A cells undergoing bone morphogenetic protein 4-mediated epithelial mesenchymal transition. Tumor Biol 36:3549–3556

Pickup MW, Hover LD, Guo Y, Gorska AE, Novitskiy SV, Moses HL, Owens P (2015) Deletion of the BMP receptor BMPR1a impairs mammary tumor formation and metastasis. Oncotarget 6:22890–22904

Qi X, Li TG, Hao J, Hu J, Wang J, Simmons H, Miura S, Mishina Y, Zhao GQ (2004) BMP4 supports self-renewal of embryonic stem cells by inhibiting mitogen-activated protein kinase pathways. Proc Natl Acad Sci USA 101:6027–6032

Reungwetwattana T, Weroha SJ, Molina JR (2012) Oncogenic pathways, molecularly targeted therapies, and highlighted clinical trials in non-small-cell lung cancer (NSCLC). Clin Lung Cancer 13:252–266

Richter A, Valdimarsdottir L, Hrafnkelsdottir HE, Runarsson JF, Omarsdottir AR, Oostwaard DW, Mummery C, Valdimarsdottir G (2014) BMP4 promotes EMT and mesodermal commitment in human embryonic stem cells via SLUG and MSX2. Stem Cells 32:636–648

Robert B (2007) Bone morphogenetic protein signaling in limb outgrowth and patterning. Dev Growth Differ 49:455–468

Rothhammer T, Poser I, Soncin F, Bataille F, Moser M, Bosserhoff AK (2005) Bone morphogenic proteins are overexpressed in malignant melanoma and promote cell invasion and migration. Cancer Res 65:448–456

Sadlon TJ, Lewis ID, D'Andrea RJ (2004) BMP4: its role in development of the hematopoietic system and potential as a hematopoietic growth factor. Stem Cells 22:457–474

Schneider CA, Rasband WS, Eliceiri KW (2012) NIH image to imagej: 25 years of image analysis. Nat Methods 9:671–675

Shepherd TG, Nachtigal MW (2003) Identification of a putative autocrine bone morphogenetic protein-signaling pathway in human ovarian surface epithelium and ovarian cancer cells. Endocrinology 144:3306–3314

Shirai YT, Ehata S, Yashiro M, Yanagihara K, Hirakawa K, Miyazono K (2011) Bone morphogenetic protein-2 and -4 play tumor suppressive roles in human diffuse-type gastric carcinoma. Am J Pathol 179:2920–2930

Su D, Zhu S, Han X, Feng Y, Huang H, Ren G, Pan L, Zhang Y, Lu J, Huang B (2009) BMP4-Smad signaling pathway mediates adriamycin-induced premature senescence in lung cancer cells. J Biol Chem 284:12153–12164

Thawani JP, Wang AC, Than KD, Lin CY, La Marca F, Park P (2010) Bone morphogenetic proteins and cancer: review of the literature. Neurosurgery 66:233–246

Virtanen S, Alarmo EL, Sandström S, Ampuja M, Kallioniemi A (2011) Bone morphogenetic protein-4 and -5 in pancreatic cancer–novel bidirectional players. Exp Cell Res 317:2136–2146

Winnier G, Blessing M, Labosky PA, Hogan BL (1995) Bone morphogenetic protein-4 is required for mesoderm formation and patterning in the mouse. Genes Dev 9:2105–2116

Xu T, Yu C-Y, Sun J-J, Liu Y, Wang X-W, Pi L-M, Tian Y-Q, Zhang X (2011) Bone morphogenetic protein-4-induced epithelial-mesenchymal transition and invasiveness through Smad1-mediated signal pathway in squamous cell carcinoma of the head and neck. Arch Med Res 42:128–137

Ye XY, Niu XM, Tang NW, Xu YH, Li ZM, Yu YF, Lu S, Chen ZW (2012) Adenovirus mediated knockdown of bone morphogenetic protein 2 inhibits human lung cancer growth and invasion in vitro and in vivo. Int J Immunopathol Pharmacol 25:967–976

Yokoyama Y, Watanabe T, Tamura Y, Hashizume Y, Miyazono K, Ehata S (2017) Autocrine BMP-4 signaling is a therapeutic target in colorectal cancer. Cancer Res 77:4026–4038

Zeng S, Zhang Y, Ma J et al (2017) BMP4 promotes metastasis of hepatocellular carcinoma by an induction of epithelial–mesenchymal transition via upregulating ID2. Cancer Lett 390:67–76

Zhang J, Li L (2005) BMP signaling and stem cell regulation. Dev Biol 284:1–11

Zhang L, Ye Y, Long X, Xiao P, Ren X, Yu J (2016) BMP signaling and its paradoxical effects in tumorigenesis and dissemination. Oncotarget 7:78206–78218